

# Structural and electrical characterization of $\text{La}^{3+}$ substituted PMS-PZT (Zr/Ti:60/40) ceramics

H. MENASRA<sup>1,\*</sup>, Z. NECIRA<sup>1</sup>, K. BOUNABE<sup>1</sup>, M. ABBA<sup>1</sup>, A. MEKLID, A. BOUTARFAIA<sup>1,2</sup>

<sup>1</sup>Applied Chemistry Laboratory, Exact and Natural and Life Sciences Faculty Materials Science Department, Mohamed Kheider University of Biskra BP145 (7000), Algeria

<sup>2</sup>University of Ouargla, Ouargla, (35000) Algeria

$\text{Pb}_{(1-x)}\text{La}_x[(\text{Zr}_{0.6}\text{Ti}_{0.4})_{(1-x)}(\text{Mn}_{1/3}\text{Sb}_{2/3})_x]\text{O}_3$  ceramics with  $x = 0.02, 0.03, 0.04,$  and  $0.05$  were synthesized by using a conventional solid state reaction route. The influence of La, Mn, and Sb contents on phase structure, microstructure, and electric properties were investigated. The results of X-ray diffraction (XRD) show that the phase structure of the ceramics transforms from rhombohedral phase to tetragonal phase. However, the minority pyrochlore phase appears on the micrographs of XRD and SEM if the doping concentration is greater than 2 mol%. The grain size of the ceramics gradually increases (from 1.36  $\mu\text{m}$  to 1.57  $\mu\text{m}$ ) with increasing doping. The dielectric properties of the ceramics have been measured as a function of temperature in the range of 20 °C to 430 °C at 1 kHz. The results indicate that the transition temperature and the maximum dielectric constant decrease with increasing PL-PMS content in the system. These results clearly show the significance of PL-PMS in controlling the dielectric behavior of the PL-PMS-PZT system.

Keywords: *PZT ceramics; PMS; pyrochlore phase; diffusivity*

## 1. Introduction

For a long time, a large number of research has been focused on lead zirconate titanate solid solution (PZT) because of its interesting practical application such as actuators, transducers, sensors and pyroelectric detectors [1–4]. PZT ceramics have been extensively modified (doped) with small amount of different additives that made them more attractive for any specific application. Such kind of modification is classified as “soft” or “hard” by differentiating the cases when the dopant ion has higher or lower valence than the targeted one in the  $\text{ABO}_3$  perovskite cell [5–11]. It has been well established that La-modified PZT has tremendous electrical and electromechanical applications in research as well as in industry [12–14].

From the literature survey of PLZT materials, it has been found that suitable substitution at Pb/La and/or Zr/Ti sites in different ratios can modify their electric, piezoelectric

and pyroelectric properties [15]. Researchers have paid a lot of attention to co-doping of PZT with Mn and Sb (noted PMS-PZT) ceramics since it displayed significantly higher electromechanical coupling factors [16–20]. For example, the effect of rare-earth substitutions in PMS-PZT ceramics was studied by Yoon et al. [21] and later by Gao et al. [22], but the effects of combined additions of Mn and Sb ions on PLZT ceramics have not been studied at all. In view of the above, we have studied the effect of Mn and Sb co-doping on structural and dielectric properties of PLZT (Zr/Ti:60/40) ceramics, which is reported here.

## 2. Experimental

The ceramic samples were prepared through a high temperature solid-state reaction technique [23] in the following conditions: charge neutrality and tolerance factor [4, 25]. High purity raw materials ( $\text{Pb}_3\text{O}_4$ ,  $\text{ZrO}_2$ ,  $\text{TiO}_2$ ,  $\text{La}_2\text{O}_3$ ,  $\text{MnO}_2$  and  $\text{Sb}_2\text{O}_3$ ) were stoichiometrically weighed according to the composition  $\text{Pb}_{(1-x)}\text{La}_x[(\text{Zr}_{0.6}\text{Ti}_{0.4})_{(1-x)}(\text{Mn}_{1/3}\text{Sb}_{2/3})_x]\text{O}_3$  to

\*E-mail: hayetmenasra@yahoo.com

obtain  $x = 2$  mol%, 3 mol%, 4 mol% and 5 mol%. From now, we shall refer to this compounds as PZT – xPMS + xLa or  $x = 2$  mol%, 3 mol%, 4 mol% and 5 mol%. The batch powders were dispersed in acetone and mixed by a magnetic stirrer for two hours. The obtained paste was dried at 80 °C, and then crushed in a glass mortar for 4 hours. The powders were calcined at 900 °C for 2 h at a heating rate of 2 °C/min. The calcined powders were crushed in a similar manner to the first crushing but for 6 hours, for better size reduction. A 5 % polyvinyl alcohol (PVA) water solution was used as a binder to increase the plasticity of the powders. The weight ratio of the PVA solution and the powders was 1:20. The powder and PVA solution were mixed in a mortar and then uniaxially pressed into pellets at a pressure of 200 MPa in a cylindrical stainless steel die using a hydraulic press. The size of those pellets was 13 mm in diameter; while their thickness was 1 mm. The pellets were packed into crucibles covered with alumina cover. The inner space of the crucibles was filled with the powders of  $\text{PbZrO}_3$  in order to prevent intensive evaporation of the lead during the sintering. A typical sintering schedule included heating to 1150 °C for 120 minutes at a heating rate of 2 °C/min and natural cooling in the furnace.

Powder X-ray diffraction was recorded by X-ray powder (BRUKER-AXE, D8) diffractometer using  $\text{CuK}\alpha$  radiation ( $\lambda = 1.5406 \text{ \AA}$ ) in a wide range of Bragg angles ( $20^\circ \leq 2\theta \leq 60^\circ$ ). Densities of sintered samples were calculated from the sample dimensions and weight. Microstructural features such as a grain size and pores were characterized by means of scanning electron microscopy (SEM: JEOL JSM-6390LV) [11].

Sintered pellets were coated with silver to form an electric contact and fired at 750 °C for forty five minutes, before using for any electrical measurements. The dielectric permittivity and loss tangent of the sintered samples at 1150 °C were measured as a function of frequency at different temperatures (room temperature to 400 °C) using LCR meter (Good Will Instrument Co., Ltd.).

## 3. Results and discussion

### 3.1. XRD results

The room temperature (RT) X-ray diffractogram of the PZT – xPMS + xLa perovskite ceramics sintered at 1150 °C has been presented in Fig. 1. The observed X-ray diffraction peaks are sharp and single, and they are different from the patterns of the ingredients. This confirms the good homogeneity and crystallization of the prepared sample. The XRD data have been analyzed by comparing with the JCPDS Card No. 53785 for the rhombohedral and 46-0504 for the tetragonal phases of PLZT ceramics. The XRD patterns of the ceramics, in the range of  $2\theta$  from  $40^\circ$  to  $50^\circ$ , show a change in the (2 0 0) reflection with the concentration of La, and PMS in the specimens. It is seen from this figure that the maximum emission peak for (2 0 0) is achieved at  $x < 5$  mol% of La, and PMS in accordance with the rhombohedral cell, and is split to (0 0 2) and (2 0 0) at 5 mol% La and PMS in accordance with the tetragonal cell pattern. The transformation from rhombohedral to tetragonal phase can be attributed to the fact that introduction of  $\text{La}^{3+}$ , the ionic radius of which is smaller than that of  $\text{Pb}^{2+}$ , in the A-site induces lattice distortion, reducing the cell volume with shortened a-axis and c-axis in the perovskite structure [9, 26–28]. As the La, PMS concentrations increase, the ceramic system gradually changes from rhombohedral to tetragonal phase probably approaching towards the morphotropic phase boundary (MPB = R + T) region. Lattice parameters were assessed using  $d_{hkl}$  values calculated from XRD patterns of the pellets sintered at 1150 °C (Table 1). However, there is an additional peak (for  $x > 2$  mol%) usually referred as secondary or pyrochlore phase [29, 30]. The relative amount of the pyrochlore phase to the perovskite phase was estimated using the following peak intensity ratio equation [31]:

$$\text{pyrochlore } \% = \frac{I_{\text{pyro.}}}{I_{\text{pyro.}} + I_{(110)}} \times 100 \quad (1)$$

where  $I_{\text{pyro.}}$  and  $I_{(110)}$  are the intensities of the pyrochlore peak and the (1 1 0) perovskite phase. The pyrochlore values are found to increase with

increasing ions additions (from 3 % to 6 %), which is in agreement with the value reported for doped PZT [32].

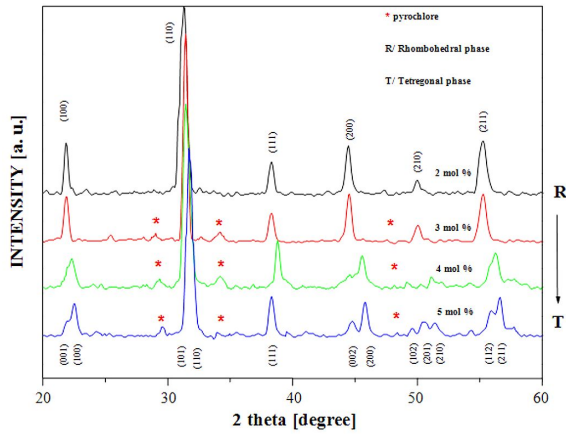


Fig. 1. XRD patterns of PZT – xPMS + xLa ceramics sintered at 1150 °C.

### 3.2. SEM analysis

SEM micrographs of the sintered samples are shown in Fig. 2. The sintered pellets have been found to have a grain size of the order of  $\sim 2.28 \mu\text{m}$  and uniform grain distribution, which is in accordance with the value shown in Table 1. On the other hand, the secondary pyrochlore phase is clearly present on the micrographs as cubic particulates [33, 34] (Fig. 2c and Fig. 2d) but PLZT phase as spherical particulates. The average grain size was determined directly from the SEM micrographs by using the classical linear interception method.

### 3.3. Dielectric properties

Fig. 3 shows the variation of the dielectric constant  $\epsilon_r$  as a function of temperature at frequency of 1 kHz for all ceramics sintered at 1150 °C. Similar to other ferroelectrics, the dielectric constant of PZT – xPMS + xLa increases progressively with a rise in temperature up to its maximum value  $\epsilon_{\text{max}}$  at a particular temperature (called  $T_c$ ) and then decreases, indicating the phase transition in the compounds. The dielectric peaks are found slightly broadened for  $x > 2 \text{ mol}\%$  and sharp for  $x = 2 \text{ mol}\%$ . The broadened peaks indicate that

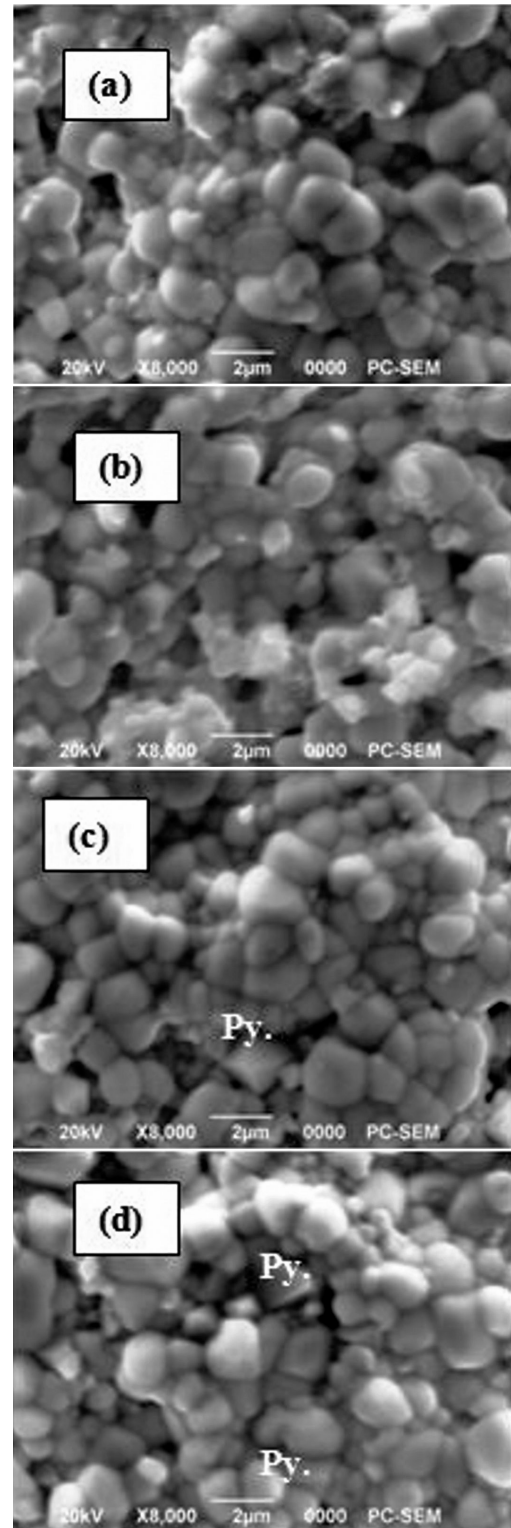


Fig. 2. SEM micrographs of pyrochlore (Py) and PZT – xPMS + xLa pellets (a)  $x = 0.02$ , (b)  $x = 0.03$ , (c)  $x = 0.04$ , (d)  $x = 0.05$ , sintered at 1150 °C.

Table 1. Comparison of lattice parameters, volume and average grain size of PZT – xPMS + xLa ceramics.

Composition	System (rhombohedral)			Density [g/cm <sup>3</sup> ]	Average grain size [μm]	
	a [Å]	α [°]	V [Å <sup>3</sup> ]			
PZT – 2 % PMS+2 % La	4.0528	89.76	66.57	7.32	1.36	
PZT – 3 % PMS+3 % La	4.0624	89.69	67.04	7.46	1.38	
PZT – 4 % PMS+4 % La	4.0852	88.96	69.17	7.61	1.44	
Composition	System (tetragonal)				Density [g/cm <sup>3</sup> ]	Average grain size [μm]
	a = b	c	c/a	V [Å <sup>3</sup> ]		
PZT – 5 % PMS + 5 % La	3.9653	4.052	1.0218	63.71	7.44	1.57

the phase transition is of diffuse type, which is an important characteristic of disordered and distorted perovskite materials. The broadening of the peak is attributed to disordering in the arrangement of cations at the A-site (La<sup>3+</sup>) and/or B-site (Mn<sup>4+</sup> and Sb<sup>3+</sup>) leading to a microscopic heterogeneity in the composition, and/or scattering mechanism where the scattering cross-section depends on the grain size and/or the inter-grain spacing [35].

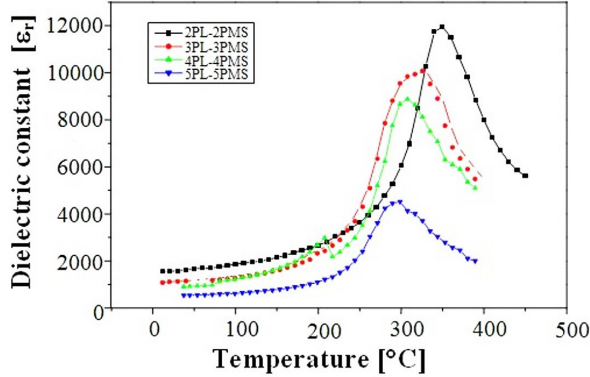


Fig. 3. Variation of dielectric constant with temperature at 1 kHz for PZT – xPMS + xLa samples sintered at 1150 °C.

Fig. 4 shows the change in dielectric loss ( $\tan\delta$ ) as a function of temperature at 1 kHz. For the all compositions sintered at 1150 °C, as temperature increases, loss tangent is almost constant up to 300 °C, but then it starts increasing with temperature. This increase in  $\tan\delta$  may be due to an increase in the electrical conduction of the residual current and absorption current [36].

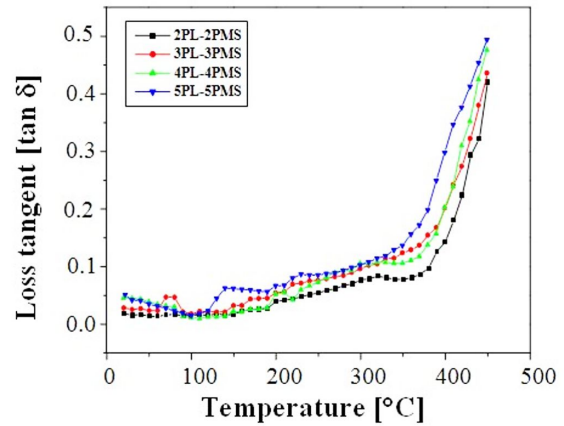


Fig. 4. Variation of dielectric loss with temperature at 1 kHz for PZT – xPMS + xLa samples sintered at 1150 °C.

The values of dielectric constant and  $\tan\delta$  at RT and  $T_c$  are given in Table 2. The degree of disorder of the PZT – xPMS + xLa can be described by a modified Curie-Weiss relationship [37] where  $\gamma$  and  $C$  are assumed to be constant:

$$\frac{1}{\epsilon} - \frac{1}{\epsilon_{max}} = \frac{(T - T_c)^\gamma}{C} \quad 1 \leq \gamma \leq 2 \quad (2)$$

The parameter  $\gamma$  gives information on the character of phase transition: for  $\gamma = 1$ , a normal Curie-Weiss law is valid,  $\gamma = 2$  describes a complete diffuse phase transition (DFT) [38]. Fig. 5 shows the plot of  $\ln((1/\epsilon) - (1/\epsilon_{max}))$  versus  $\ln(T - T_c)$  at 1 kHz for PLZTMS sample. Linear relationships were obtained. The slopes of the fitting curves were used to determine the parameter  $\gamma$ . The values of  $\gamma$  are listed in Table 2. It can be seen an increase

Table 2. Physical parameters and diffusivity  $\gamma$  of PZT – xPMS + xLa pellets sintered at 1150 °C.

Composition	Room temperature [RT]		Tc		$\gamma$
	$\epsilon$	$\tan\delta$	$\epsilon_{\max}$	$\tan\delta$	
PZT – 2 % PMS + 2 % La	1564.02	0.0182	11950.21	0.077	1.63
PZT – 3 % PMS + 3 % La	1114.36	0.0282	10081.95	0.113	1.28
PZT – 4 % PMS + 4 % La	922.30	0.0457	8876.51	0.104	1.39
PZT – 5 % PMS + 5 % La	535.69	0.0508	4515.92	0.102	1.54

( $x > 0.02$ ) in the value of  $\gamma$  with La and PMS concentrations indicating an increase in diffusivity.

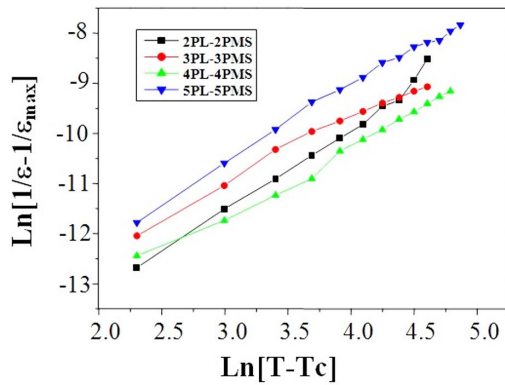


Fig. 5.  $\ln(1/\epsilon - 1/\epsilon_{\max})$  vs.  $\ln(T - T_c)$  of PZT – xPMS + xLa ceramics at 1 kHz.

## 4. Conclusions

PZT – xPMS + xLa ceramics have been prepared using solid-state reaction technique and their structural and dielectric properties were investigated. Addition of La and PMS seems to enhance crystallization of the raw powders in the rhombohedral phase for  $x = 2$  mol%, 3 mol%, and 4 mol% but in the tetragonal phase for  $x = 5$  mol%. Moreover, the secondary phase has been detected in ceramics with  $x > 2$  mol%; it increased with increasing ion doping. Grains with the size ranging from 1.36  $\mu\text{m}$  to 1.57  $\mu\text{m}$  and uniform grain distribution were obtained which is confirmed by the density of the ceramics. The decrease in transition temperature and dielectric constant can be attributed to lead vacancies creation by donor cation ( $\text{La}^{3+}$ ), and acceptor cations ( $\text{Mn}^{4+}$  and  $\text{Sb}^{3+}$ ) to reduce

the oxygen vacancies mobility and balance the charge in the modified PZT. The decreasing of diffusivity  $\gamma$  of the compounds with  $x > 2$  mol% indicates some degree of disordering in the system.

## References

- [1] JAFFE B., ROTH R.S., MARZUL L.S., *J. Res. Natl. Bur. Stand.*, 55 (1955), 239.
- [2] UCHINO K., *Ceram. Int.*, 21 (1995), 309.
- [3] JAFFE B., COOKJR W.R., JAFFE H., *Piezoelectric Ceramics*, Academic Press, New York, 1971, p. 317.
- [4] HAERTLING G.H., *J. Am. Ceram. Soc.*, 82 (1999), 797.
- [5] JAFFE B., ROTH R.S., MARZULL S., *J. Appl. Phys.*, 25 (1954), 809.
- [6] GULLO-LOPEZ F.A., CARBRERE J.M., AGULLO-RUEDA F., *Electro Optics Phenomena, Materials and Applications*, Academic Press INC, San Diego, 1994, p. 146.
- [7] DUTTA S., CHOUDHARY R.N.P., *Appl. Phys. A-Mater.*, 90 (2008), 323.
- [8] PARASHAR S.K.S., CHOUDHARY R.N.P., MURTY B.S., *J. Appl. Phys.*, 98 (2005), 104305.
- [9] KUMAR A., MISHRA SK., *Inter. J. Miner. Metall. Mater.*, 21 (2014), 1019.
- [10] RAI R., SHARMA S., CHOUDHARY R.N.P., *J. Mater. Sci.*, 41 (2006), 4259.
- [11] MENASRA H., NECIRA Z., BOUNABE K., MAK-LIDE A., BOUTARFAIA A., *MSA*, 4 (2013), 293.
- [12] HAERTLING G.H., *J. Am. Ceram. Soc.*, 5 (1971), 303.
- [13] NOVAK N., PIRCR., KUTNJAKZ., *Eur. Phys. Let.*, 102 (2013), 17003.
- [14] WAKINO K., MINAL K., TAMURA H., *J. Am. Ceram. Soc.*, 67 (1984), 278.
- [15] DUTTA S., CHOUDHARY R.N.P., *Ferroelectrics*, 330 (2006), 75.
- [16] LONG J., CHEN H., MENG Z., *Mater. Sci. Eng. B-Adv.*, 99 (2003), 445.
- [17] ZHU Z.G., LI G.R., XU Z.J., ZHANG W.Z., YIN Q.R., *J. Phys. D Appl. Phys.*, 38 (2005), 1464.
- [18] HONG-LIANG D., ZHI-BIN P., ZHI-MIN L., FA L., DONG-MEI Z., WAN-CHENG Z., SHAO-BO Q., *Trans. Nonferrous Met. Soc. China*, 16 (2006), 165.
- [19] SAKAKI C., NEWALKAR B.L., KOMARNENI S., *Jpn. J. Appl. Phys.*, 40 (2001), 6907.

- [20] VOLNAN K., *Ph.D. Thesis*, Middle East Technical University, Turkey, 2011.
- [21] YOON J., KANG H.W., KUCKEIKO S.I., JUNG H.J., *J. Am. Ceram. Soc.*, 81 (1998), 2474.
- [22] GAO Y.K., UCHINO K., VIEHLAND D., *J. Appl. Phys.*, 92 (2002), 2094.
- [23] RAI R., MISHRA S., SINGH N.K., *J. Alloy. Compd.*, 487 (2009), 494.
- [24] YAN Q.F., LI Q., ZHANG Y.L., *J. Inorg. Mater.*, 16 (2001), 649.
- [25] GOLDSCHMIT V.M., *Geochem. Vert. Elem.*, 7 (1972), 8.
- [26] XU Y.H., *Ferroelectric and Piezoelectric Materials*, Science Press, Beijing, 1978, p. 332.
- [27] DENG G., YIN Q., DING A., ZHENG X., CHENG W., QIU P., *J. Am. Ceram. Soc.*, 88 (2005), 2310.
- [28] LAISHRAM R., THAKUR O.P., BHATTACHARYA D.K., HARSH, *Mater. Sci. Eng. B-Adv.*, 172 (2010), 172.
- [29] CARIM A.H., TUTTLE B.A., DAGHTY D.H., *J. Am. Ceram. Soc.*, 74 (1974), 1455.
- [30] LIAN J., WANG L., CHEN J., SUN K., EWING R.C., MATT FARMER J., BOATNER L.A., *Acta Mater.*, 51 (2013), 1493.
- [31] DAI X., VIECHLAND Z.D., *J. Am. Ceram. Soc.*, 79 (1995), 1957.
- [32] PELAIZ-BARRANCO A., *Ph.D. Thesis*, Havana University, Cuba, 2001
- [33] YIMNIRUN R., ANANTA S., LAORATANAKUL P., *J. Am. Ceram. Soc.*, 25 (2005), 3235
- [34] YIMNIRUN R., MEECHOOWAS E., ANANTA S., TUNKASIRI T., *Chiang Mai Univ. J.*, 3 (2004), 2
- [35] ROLOV B. N., *Soviet Phys. Solid State*, 6 (1965), 1676
- [36] TAREEV B., *Physics of dielectric materials*, Mir Publisher, Moscow, 1979, p. 157
- [37] KOVAL V., ALEMANY C., BRIANCIN J., BRUNCKOVA H., *J. Electroceram.*, 10 (2003), 19
- [38] SMOLENSKII G.A., *J. Phys. Soc. Jpn.*, 28 (1970), 26.

Received 2016-06-22

Accepted 2018-03-17